JOURNAL OF AVIATION

e-ISSN: 2587-1676 J Aviat 2021; 5(2): 72-81

Research Article DOI : 10.30518/jav.943804

Design, Modelling and Control of an Eight-Rotors UAV with Asymmetric Configuration for Use in Remote Sensing Systems

*Nihat ÇABUK[1]**, *Şahin YILDIRIM [2]*

[1]Aksaray University, Technical science Vocational school, Aksaray, Turkey
[2] Mechatronic Engineering Department, Faculty of Engineering, Erciyes University, Kayseri, Turkey

Abstract

The use of multirotor unmanned aerial vehicles (UAV), which can take-off and landing vertically, is gradually expanding. Although there are many types of these vehicles with standard configuration, non-standard configurations may be required for special purposes usage. So, an octocopter UAV with asymmetric configuration is proposed in this study. In particular, this asymmetrically configured octocopter is intended to be used for imaging or mapping purposes, and may be a solution to widen the viewing angle of the camera or any sensor placed on the vehicle, especially in the use of multiple cameras and sensors. The mathematical model of this proposed UAV system was obtained and the trajectory tracking was performed using PID control method. The control parameters of the controller were determined using Grey Wolf Optimizer (GWO). Considering the propellers determined in two different sizes due to its asymmetrical structure, it has been observed that the proposed UAV performs a satisfactory trajectory tracking.

Keywords: Asymmetric UAV, Design, PID Control, GWO Optimization, Remote Sensing

1. Introduction

Unmanned aerial vehicles (UAVs) use areas and numbers are increasing day by day. They are designed and produced for different purposes [1–4]. Hassanalian and Abdelkefi [5], conducted extensive research on the use of drones and their uses. In the study, they have realized a different classification of UAV from very large to very small size ones, which have wings with fixed, flapping or rotary. They also examined the design difficulties of each type of drone in this study, which was also compared in terms of weight and flight range.

Especially, multirotor UAVs capable of vertical landing and take-off have taken their place among today's widely used vehicles. So far, a lot of studies have been done on these vehicles. These studies are generally related to control of vehicles with the four-rotors, six-rotors and eight-rotors with

Corresponding Author: Nihat Çabuk nihatcabuk@aksaray.edu.tr
Citation: Çabuk N., Yıldırım Ş. (2021). Design, Modelling and Control of an Eight-Rotors UAV with Asymmetric Configuration for Use in Remote Sensing Systems J. Aviat. 5 (2), 72-81.
ORCID: [1] https://orcid.org/0000-0002-3668-7591 ; [2] https://orcid.org/0000-0002-7149-3274
DOI: https://doi.org/10.30518/jav.943804
Received: 27 May 2021 **Accepted:** 11 September 2021 **Published (Online):** 20 December 2021

standard configuration [6–8]. Apart from these, studies have been carried out on the design of the vehicles with some different configurations [9] or interchangeable configurations. Niemiec et al. [10] proposed a model with interchangeable rotor structure between four and ten rotors. In the study, the four-rotors model comparison in terms of power requirement to others is better for the hover position, but they have expressed worse results for forward motion. Brischetto et al. [11] proposed a multirotor UAV model that can be changed between three and eight rotors. In addition to this, there are also some studies including various solution suggestions where there are internal and external disruptive effects such as rotor faults and wind [12,13]. Merheb et al. [14] developed an emergency fault-tolerant controller for quadrotor suffering a total loss of one of its rotors. It was transformed into a different system able to be controlled using only three rotors. According to the result, they expressed that the trirotor able to follow a path, but with slow variation of the yaw rate. As the popularity of UAVs increases, it is necessary to obtain different configurations for different usage areas [15,16] such as remote sensing applications [17,18]. In terms of imaging, it is used for many purposes such as agricultural monitoring [19–21], road [22,23], film and photographic industry and monitoring of industrial plants etc. [24–27]. Vijayanandh at al.[28] designed and simulated a hexacopter to surveillance for forest areas. Zakeri at al. [29] used a quadrotor UAV as digital imaging system for collecting asphalt surface data on a distressed area for interpretation of visual conditions. Streßer at al. [30] used a four-rotor UAV to estimate surface current fields off-the-shelf over a river. Liu et al. [31] proposed a multirotor air vehicle system for cyanobacterial harmful algal blooms monitoring. In view of the studies conducted, multi-rotor unmanned air vehicles designed for imaging purposes are preferred because they have completed the monitoring tasks at a lower cost and in less time. In another study [32], remote soil moisture measurement was made with sensors mounted on the drone. In order for the vehicles to perform these tasks well, the sensors to remote sensing [33] and camera or multi camera and sensor [34,35] should be positioned in such a way that they can receive images at a wider angle. In these vehicles, it can be said that the parts that narrow the view of the camera are arms, motors and propellers. Therefore, for better imaging, either the camera should be mounted in a very convenient location or the mechanical design of the air vehicle should be changed in the classical configuration.

For these reasons, in this study, an octocopter UAV with asymmetric configuration was designed for remote sensing such as imaging, mapping and etc tasks. Thus, it is aimed to show that a multirotor UAV can be used for special purposes with non-standard configuration. The flight simulation was performed the proposed octocopter. In the simulation, PID controller was used and the controller parameters were tuned using Gray Wolve Optimization (GWO).

This study is structured as summarized follows. Section 2 is about remote sensing concept, introducing the physical properties of the UAV and obtaining the mathematical model based on these properties. Besides, in the section, process of controller design and GWO are explained. Section 3 is about simulation. In this section, controller parameters are tuned and the octocopter UAV is simulated. Obtained results are discussed in section 4. Finally, explanations about conclusion and future works were given in section 5.

2. **Materials and Methods**

In this section, the introduction of the physical properties of the octocopter with asymmetric configuration and obtaining the mathematical model according to these properties are presented. Then, the controller structure used and the algorithm used in the optimization of controller parameters are introduced.

2.1. Remote Sensing Concept

Figure 1. Some sensors used in UAVs for remote sensing

Remote sensing, refers mostly to any noncontact sensing technique by the object space can be observed. Generally, the remote sensing has been used for satellite and airborne platforms, acquiring

data typically by optical and radar sensors. For remote sensing purposes, there are sensors

Remote sensing systems for UAVs

Active sensing systems	Passive sensing systems
• Laser altimeter	• Accelerometer
• Lidar	• Hyperspectral radiometer
• Radar	• Imaging radiometer
• Ranging Instrument	• Sounder
• Scatterometer	• Spectrometer
• Sounder	• Spectroradiometer

commonly used in unmanned aerial vehicles such as multispectral cameras, RGB cameras, thermal infrared sensors, hyperspectral sensors and lidar. These sensors, which have various spectral ranges, can be of different weights [33]. Those with less weight are more preferred in unmanned aerial vehicles. However, in addition to the advantage that the lower weight provides to the UAV, it causes the limitation of the features of these sensors. Thus, the measurements made may not be as desired. This negative situation is partially compensated by the advantage of using the UAV in ground conditions that are not suitable for land operation. There are two main types of remote sensing systems, active and passive. In the active remote sensing system, the energy required for detecting objects is supplied from the sensors, while in passive systems, the reflection of the energy provided by natural energy sources from the objects is detected by the sensors. Active and passive remote sensing systems are schematized below [36].

In remote sensing systems where, multiple sensors can be used, it may be important to find a suitable and sufficient location for the placement of sensors on UAVs. In Figure 1, it is seen some sensors and UAV image. The image is taken from [37].

2.2. Modelling of the Octocopter UAV

The mechanical design of the octocopter with asymmetric configuration have presented in this section. Some assumptions in the mechanical design of the proposed UAV system in accordance with the scenario set up in this study are given below.

•It should be able to carry the sensor group with a total mass of 5 kg.

•It must have a different configuration than the standard UAV configuration to create more options for the placement of the sensors.

•The resulting non-standard configuration should not have a physical structure that would affect the UAV's flight mission.

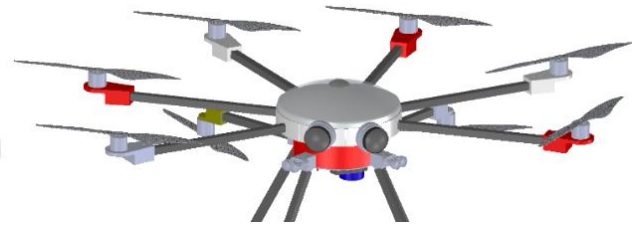

Figure 2. CAD model of the octocopter with asymmetric configuration with sensors

Based on these assumptions, the computer aided design model (CAD) of the proposed asymmetric UAV and the physical parameters of this model are given in Figure 2 and Figure 3, respectively.

The solid model of the asymmetric UAV with eight rotors, with six rotors in the upper plane and two in the lower plane, is given in Figure 2. Thus, as seen in Figure 3, it is obtained with a non-standard UAV designed with wide a 135° angle.

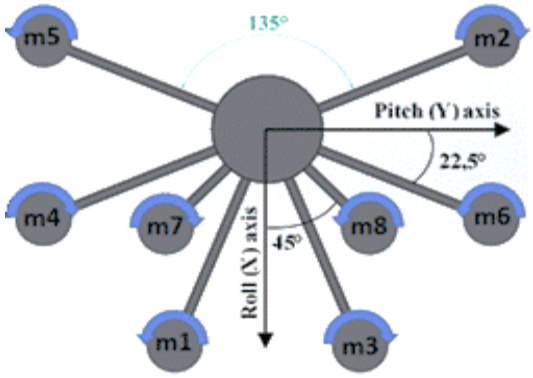

Figure 3. Physical parameters of the octocopter

The physical parameters of the octocopter UAV with asymmetric configuration are given in Table 1. Using these physical parameters, the mathematical model of the UAV is obtained.

Table 1. Physical parameters of the octocopter UAV

Descriptions	Value
Length of arms on upper plane [l_1]	660 mm
Length of arms on lower plane [l_2]	450 mm
Thrust constant of couple of rotor-propeller for 12 inches propeller [k_{f1}]	$0{,}22x10^{-4}\frac{N}{(rad/sec)^2}$
Thrust constant of couple of rotor-propeller for 18 inches propeller [k_{f2}]	$1{,}04x10^{-4}\frac{N}{(rad/sec)^2}$
Reverse torque constant of couple of rotor-propeller for 12 inches propeller [k_{m1}]	$0{,}9x10^{-6}\frac{Nm}{(rad/sec)^2}$
Reverse torque constant of couple of rotor-propeller for 18 inches propeller [k_{m2}]	$4.05x10^{-6}\frac{Nm}{(rad/sec)^2}$
Angle of the arm on the upper plane with pitch or roll axes	22,5°
Angle of the arm on the upper plane with pitch or roll axes	45°
Total mass of the octocopter UAV [m]	8 kg
2. and 5. propellers diameter	18"
Maximum thrust force of 2. and 5. motors [T_2]	57 N
1, 3, 4, 6, 7 and 8. propellers diameter	12"
Maximum thrust force of 1, 3, 4, 6, 7 and 8. motors [T_1]	27 N

Rotational movement of the rotor and propeller pair creates forces and moments affecting the octocopter. The effects are proportional to the rotational velocities of rotors. The equation used to calculate the moment and force required for UAV is

$$\boldsymbol{U_d} = \boldsymbol{C}\,\boldsymbol{\Omega}. \tag{1}$$

Control vector is

$$\boldsymbol{U_d} = [T \quad M_r \quad M_p \quad M_y]^T, \tag{2}$$

where, T is total maximum thrust force, which is calculated as $T = 6T_1 + 2T_2$. In this design, this value is 256 newtons, which should be approximately twice the payload of the UAV.

M_r, M_p and M_y roll, pitch and yaw moments. These moments and thrust are generated by angular velocities of rotors-propeller pairs. Angular velocities vector of rotors is

$$\boldsymbol{\Omega} = [\Omega_1^2 \quad \Omega_2^2 \quad \Omega_3^2 \quad \Omega_4^2 \quad \Omega_5^2 \quad \Omega_6^2 \quad \Omega_7^2 \quad \Omega_8^2]^T. \tag{3}$$

The relationship between these rotational velocities with the forces and moments is established by matrix C formed depending on the geometry of the octocopter. For the sake simplify $A_1 = k_{f1}l_1$, $A_2 = k_{f1}l_2$, $A_3 = k_{f2}l_1$ $s = sin$ and $c = cos$ cos abbreviations were made in the matrix is

$$C = \begin{bmatrix} k_{f1} & k_{f2} & k_{f1} & k_{f1} \\ -A_1\,s(22{,}5) & A_3\,c(22{,}5) & A_1\,s(22{,}5) & -A_1\,c(22{,}5) \\ -A_1\,c(22{,}5) & A_3\,s(22{,}5) & -A_1\,c(22{,}5) & -A_1\,s(22{,}5) \\ k_{m1} & -k_{m2} & -k_{m1} & -k_{m1} \\ k_{f2} & k_{f1} & k_{f1} & k_{f1} \\ -A_3\,c(22{,}5) & -A_1\,c(22{,}5) & -A_2\,s(45) & A_2\,s(45) \\ A_3\,s(22{,}5) & -A_1\,s(22{,}5) & A_2\,s(45) & A_2\,s(45) \\ k_{m2} & -A_1\,s(22{,}5) & -k_{m1} & k_{m1} \end{bmatrix}, \tag{4}$$

where, k_{f1} and k_{f2} are thrust and k_{m1} and k_{m2} are reverse torque constants of rotors with 12- and 18-inches propeller, respectively. These constants are experimentally determined [38]. Simplified nonlinear models of translational motion and angular motion of the octocopter are

$$\begin{aligned} m\ddot{x} &= -(T + w_x)sin\theta, \\ m\ddot{y} &= (T + w_y)cos\theta sin\phi, \\ m\ddot{z} &= (T + w_z)cos\theta cos\phi - mg, \end{aligned} \tag{5}$$

and

$$\begin{aligned} I_x\ddot{\theta} &= M_r + w_\theta, \\ I_y\ddot{\phi} &= M_p + w_\phi, \\ I_z\ddot{\psi} &= M_y + w_\psi, \end{aligned} \tag{6}$$

respectively, where x, y, and z denote the position of the vehicle, ψ, θ, and ϕ are the yaw, pitch, and roll angles, respectively, I_j represents the inertia matrix in the j-axis, and g is the gravitational acceleration. Correspondingly, w_i, where i takes values x, y, z, ψ, θ or ϕ, denotes disturbances.

2.3. Controller Design

Traditional PID control method can be applied successfully in in the control of many systems. So, in this study, PID control method is used to control the UAV. An advantage of the controllers is that two controllers can be used together to better dynamic performance from systems. This is named cascaded PID control.

Two controllers are in cascade when they are arranged so that one regulates the set point of the other.

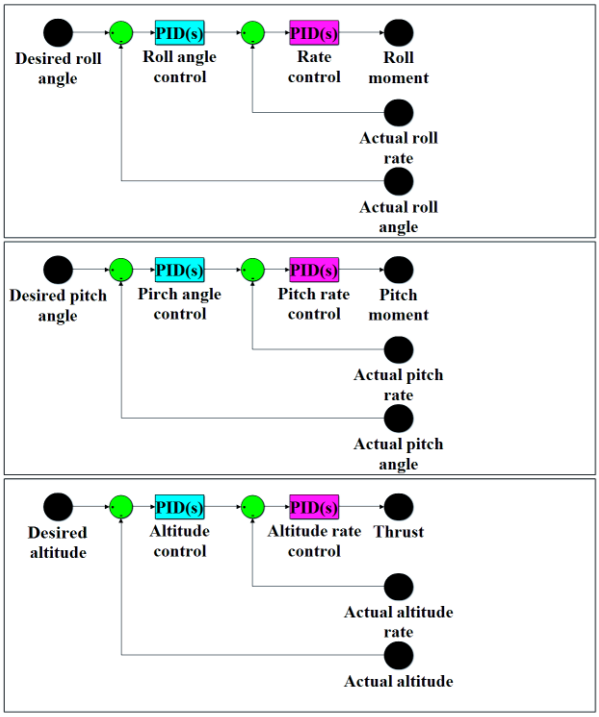

Figure 4. Cascade PID control diagram of roll, pitch and altitude

As seen in Figure 4, one controller acts as outer loop controller, which controls such as angle and level. The other controller acts as inner loop controller, which accepts the output of outer loop controller as input. In this study, proportional and derivative control is used as a PID controller. The control signal used for three variables to be controlled is

$$\begin{bmatrix} u_{thrust}(t) \\ u_{roll}(t) \\ u_{pitch}(t) \end{bmatrix} = \begin{bmatrix} k_{P,thrust}(Z_d - Z_a) - k_{D,thrust}(\dot{Z}_d - \dot{Z}_a) \\ k_{P,roll}(\theta_d - \theta_a) - k_{D,roll}(\dot{\theta}_d - \dot{\theta}_a) \\ k_{P,pitch}(\phi_d - \phi_a) - k_{D,pitch}(\dot{\phi}_d - \dot{\phi}_a) \end{bmatrix}, \quad (7)$$

where, $u_i(t)$ is control signal, Z_d, θ_d and ϕ_d are desired and Z_a, θ_a and ϕ_a actual position of altitude, roll and pitch, respectively. Similarly, $\dot{Z}_d, \dot{\theta}_d$ and $\dot{\phi}_d$ are desired and $\dot{Z}_a, \dot{\theta}_a$ and $\dot{\phi}_a$ actual speed of altitude, roll and pitch, respectively. $k_{P,i}$ is proportional and $k_{D,i}$ is derivative constant which are optimized controller parameters as seen in Table 2. Thus, the cascade PID controller can control both position and velocities of the octocopter.

2.4. Controller Parameters Optimization

Although the PID control method is a good method, if the control parameters are not determined correctly, the desired performance cannot be obtained. Thus, the controller parameters need to be tuned. There are many methods for determining PID control parameters [39–42]. The mathematical equation of the control structure used in this study is given in equation 7. So, the proportional and derivative gains of the controller are optimized as described below. Objective function formulation is crucial in optimization. Because the function is main parameter to measure the performance of the optimization technique. An optimization procedure is adopted to adjust the controller gains in the time domain. So, defined objective function is

$$J_{PD} = min \sum (a\,(t_s - t_i)^2 + b\,O_m^2), \quad (8)$$

on the time domain characteristics, where the constants denoted by a and b define the weight of the relevant parameters. t_s and t_i are the settling time and the desired settling time. O_m is defined as the Maximum Overshoot. By defined the objective function, without an overshoot a fast-settling time is aimed.

GWO, one of the meta-heuristic search algorithms, has been used to determine controller parameters in this study. The GWO is a bio inspired heuristic algorithm inspired from both the social hierarchy and hunting behavior of wolves. It has recently been proposed by [42,43]. In this algorithm, the search starts with population of randomly generated wolves which represent the solutions. During hunting optimization process, these wolves estimate the prey's location, which is optimum, through an iterative procedure.

2.5.Controller Parameters Tuning Process

In order to obtain the time domain response characteristics required to evaluate the objective function described in equation 7, the closed loop system is simulated in the Simulink environment using possible solutions determined by the GWO algorithm running in the Matlab [44,45]. In the simulation study, a step reference input is used to obtain system response. Weights a and b in the defined objective function are set to 10 and 0.5, respectively.

As optimization parameters, agent number, iteration number, lower bound and upper bound values are 30, 50, 0 and 100, respectively. Optimization is performed 10 times separately using the optimization parameters. Each optimization process is continued up to 50 iterations or until a solution reaching the $J_{PD} \leq 0.01$ condition.

Table 2. PID controller gains

States	Roll		Pitch		Altitude	
	k_P	k_D	k_P	k_D	k_P	k_D
Tuned parameters	39,58	43,54	17,80	28,26	94,51	29,75

3. Results

In order to test the usability of the designed asymmetric octocopter system, simulations for both helical and linear trajectories were performed. For the trajectory tracking performance analysis of the octocopter, three-dimensional graphics were obtained as seen in Figures 5 and 6. Besides, graphs of thrust generated by each motor-propeller pair, roll, pitch and yaw moments as seen in Figures 7-9.

3.1. Simulations of the Octocopter UAV System

The obtained tuned controller parameters are applied to the octocopter model created with Matlab Simulink. Both helical and linear trajectories determined are applied to the system as the desired input in the same simulation. During the simulation, the response of the octocopter system is fed back to the controller. The moments and force generated by the controller and physical parameters of octocopter are used to calculate the speed of the rotors (inverse kinematic). The voltage required to achieve these speeds is applied to the motors. Then, actual motor speeds are used to calculate the torque and force values that must be applied to the octocopter (forward kinematic).

The simulation was performed using both a helical and a linear trajectory for 80 seconds. During the first 40 seconds, the UAV rose and tracked the helical trajectory. For the next 40 seconds, it descends and follows a linear trajectory and lands on the ground. The three-dimensional graph of the trajectory tracking is given in the Figure 5.

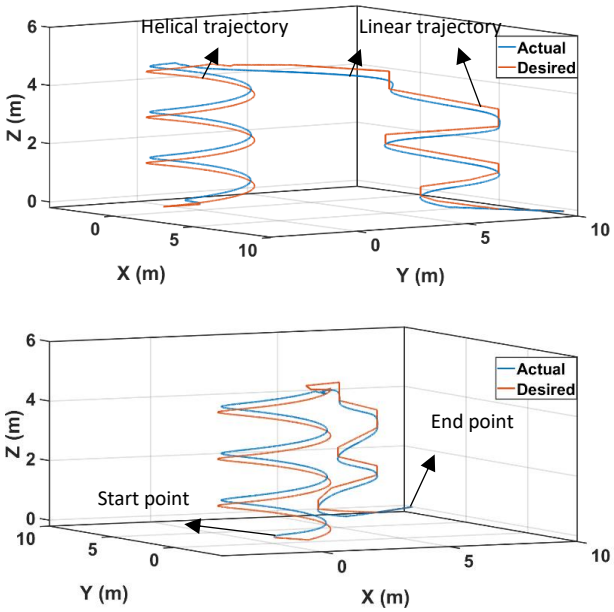

Figure 5. 3D trajectory tracking graph in two different views

Similarly, the trajectory tracking graph of each axis is given in the Figure 6.

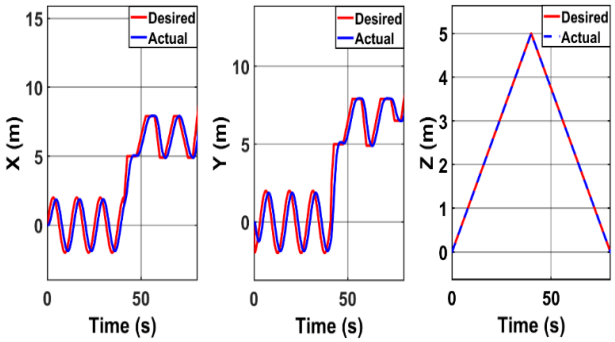

Figure 6. Trajectory tracking graph for three axes

During the simulation, thrust change produced by two motors using 18-inch and six motors using 12-inch propellers are shown in the Figure 7 and 8, respectively. The maximum thrust force that the 2nd and 5th motors can produce with 18-inch propeller is given in Table 1 as 57 newtons. It can be seen in Figure 8 that these forces are approximately 42 newtons for these two motors, tracking both linear and helical trajectory. This value corresponds to approximately 80% of the thrust that motors can generate.

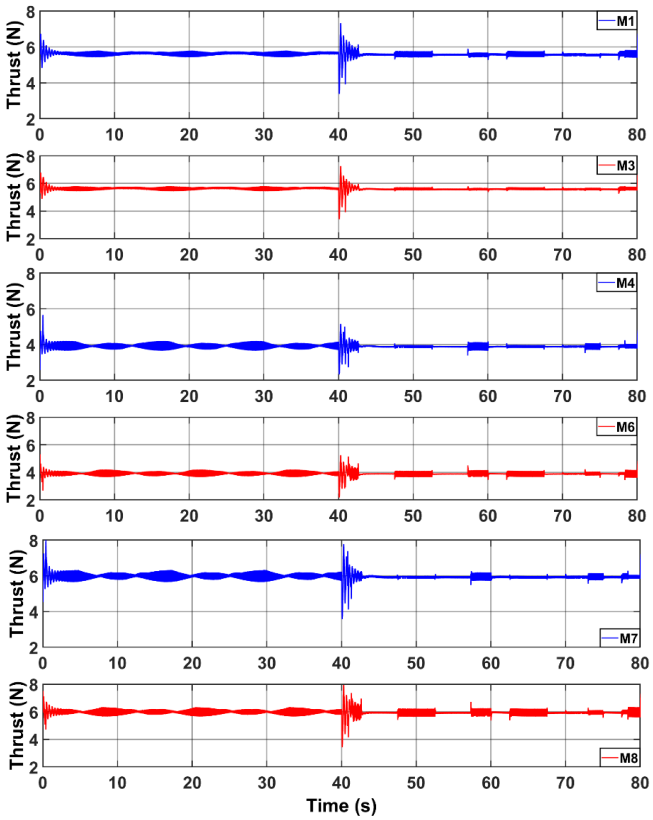

Figure 7. Thrust generation graphs of motors with 12-inches propeller

Similarly, it can be seen in Figure 8 that other motors use a maximum of about 30% of the thrust that they can generate with a 12-inch propeller for this trajectory. It is seen that both of these maximum values occur at the transition of the UAV from the helical to the linear trajectory.

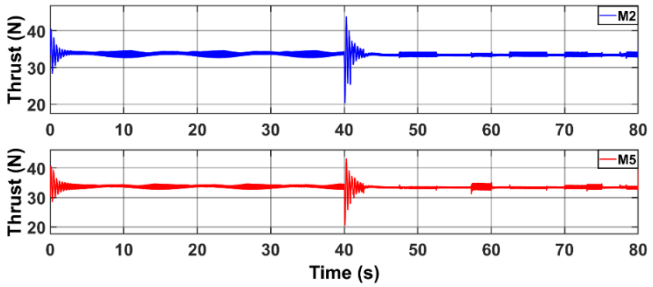

Figure 8. Thrust generation graphs of motors with 18-inches propellers

As seen in Figure 9, in the helical trajectory tracking, the forces acting on the drone body have a similar form to this trajectory, while the forms of these forces and moments are different because there are sharp turns in the linear trajectory.

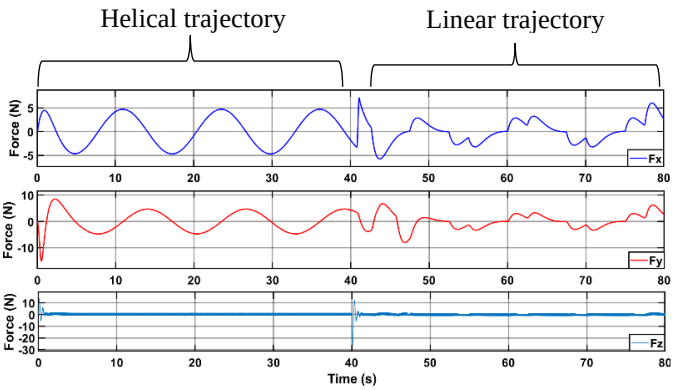

Figure 9. Net forces acting on the octocopter body in three axes.

Where, F_x, F_y, and F_z, are forces affected the octocopter body in x, y and z axis, respectively. The changes during the simulation of the net forces acting on the body of the UAV that cause the translational motion of the UAV in three axes are given in Figure 9. These values are directly related to the translational velocity and acceleration determined for the UAV.

4. Discussion

Eight-rotor UAV with asymmetric configuration was designed and controlled to use remote sensing applications. PID control method was used in this study. Optimization of control parameters was carried out using GWO. With the tuned parameters obtained, it can be said that the designed octocopter UAV has a satisfactory performance in trajectory tracking. According to the graphical results obtained, the performance of the drone in following the determined trajectory is quite satisfactory. The maximum thrust that the 2nd and 5th rotors can produce with an 18-inch propeller is 57 newtons, and for the 12-inch propeller of other rotors, this value is 27 newtons. In this simulation study, it can be said that the proposed this asymmetrical UAV model can be used for the purpose determined in this study, since the utilization rate of these thrust forces is 80% and 30%, respectively. To the best of the authors' knowledge, the results obtained in this study could not be compared with other studies, since there is no study on an asymmetrical UAV in the literature.

5. Conclusion and Future Works

Although this proposed octocopter UAV system can perform its task under normal conditions, it can be said that flight performance in more aggressive movements and situations with high external and internal disturbance will not be better than the symmetrical octocopter UAV system. In addition, if the appropriate motors and propellers are selected, a UAV model with a higher payload can be created. In future works, this proposed UAV system may be experimentally performed and controlled with a more robust and adaptive controller.

Ethical Approval
Not applicable

References

[1] S. Yu, J. Heo, S. Jeong, Y. Kwon, "Technical Analysis of VTOL UAV", J. Comput. Commun. 04 (15), 92–97, 2016.

[2] A.S. Saeed, A.B. Younes, S. Islam, J. Dias, L. Seneviratne, G. Cai, "A review on the platform design, dynamic modeling and control of hybrid UAVs", in: 2015 Int. Conf. Unmanned Aircr. Syst., IEEE, pp. 806–815, 2015.

[3] A.S. Saeed, A.B. Younes, C. Cai, G. Cai, "A survey of hybrid Unmanned Aerial Vehicles", Prog. Aerosp. Sci., 98, 91–105, 2018.

[4] Ö. Dündar, M. Bilici, T. Ünler, "Design and performance analyses of a fixed wing battery VTOL UAV", Eng. Sci. Technol. An Int. J., 23 (5), 1182–1193, 2020.

[5] M. Hassanalian, A. Abdelkefi, "Classifications, applications, and design challenges of drones: A review", Prog. Aerosp. Sci., 91, 99–131, 2017.

[6] H. Bouadi, F. Mora-Camino, "Modeling and Adaptive Flight Control for Quadrotor Trajectory Tracking", J. Aircr., 55 (2), 666–681, 2017.

[7] Y.-R. Tang, X. Xiao, Y. Li, "Nonlinear dynamic modeling and hybrid control design with dynamic compensator for a small-scale UAV quadrotor", Measurement, 109, 51–64, 2017.

[8] A.A. Najm, I.K. Ibraheem, "Nonlinear PID controller design for a 6-DOF UAV quadrotor system", Eng. Sci. Technol. An Int. J., 22 (4), 1087–1097, 2019.

[9] A. Bin Junaid, A.D.D.C. Sanchez, J.B. Bosch, N. Vitzilaios, Y. Zweiri, "Design and implementation of a dual-axis tilting quadcopter", Robotics, 7 (4), 65, 2018.

[10] R. Niemiec, F. Gandhi, R. Singh, "Control and Performance of a Reconfigurable Multicopter", J. Aircr., 55 (5), 1855–1866, 2018.

[11] S. Brischetto, A. Ciano, C.G. Ferro, "A multipurpose modular drone with adjustable arms produced via the FDM additive manufacturing process", Curved Layer. Struct., 3 (1), 202–213, 2016.

[12] M. Kuric, B. Lacevic, N. Osmic, A. Tahirovic, "RLS-based fault-tolerant tracking control of Multirotor Aerial Vehicles", in: 2017 IEEE Int. Conf. Adv. Intell. Mechatronics, IEEE, 2017: pp. 1148–1153.

[13] M. McKay, R. Niemiec, F. Gandhi, "An Analysis of Classical and Alternate Hexacopter Configurations with Single Rotor Failure", 73rd AHS Int. Annu. Forum. (2017) 1–11.

[14] A.-R. Merheb, H. Noura, F. Bateman, "Emergency Control of AR Drone Quadrotor UAV Suffering a Total Loss of One Rotor", IEEE/ASME Trans. Mechatronics, 22 (2), 961–971, 2019.

[15] L. Deng, Z. Mao, X. Li, Z. Hu, F. Duan, Y. Yan, "UAV-based multispectral remote sensing for precision agriculture: A comparison between different cameras", ISPRS J. Photogramm. Remote Sens., 146, 124–136, 2018.

[16] J.J. Sofonia, S. Phinn, C. Roelfsema, F. Kendoul, Y. Rist, "Modelling the effects of fundamental UAV flight parameters on LiDAR point clouds to facilitate objectives-based planning", ISPRS J. Photogramm. Remote Sens., 149, 105–118, 2019.

[17] G. Pajares, "Overview and current status of remote sensing applications based on unmanned aerial vehicles (UAVs)", Photogramm. Eng. Remote Sensing, 81, 281–329, 2015.

[18] C. Toth, G. Jóźków, "Remote sensing platforms and sensors: A survey", ISPRS J. Photogramm. Remote Sens., 115, 22–36, 2016.

[19] V.K. Gadi, A. Garg, S. Prakash, L. Wei, S. Andriyas, "A non-intrusive image analysis technique for measurement of heterogeneity in grass species around tree vicinity in a green infrastructure", Measurement, 114, 132–143, 2018.

[20] T. Ishida, J. Kurihara, F.A. Viray, S.B. Namuco, E.C. Paringit, G.J. Perez, Y. Takahashi, J.J. Marciano, "A novel approach

for vegetation classification using UAV-based hyperspectral imaging", Comput. Electron. Agric., 144, 80–85, 2018.

[21] J.R. Kellner, J. Armston, M. Birrer, K.C. Cushman, L. Duncanson, C. Eck, C. Falleger, B. Imbach, K. Král, M. Krůček, J. Trochta, T. Vrška, C. Zgraggen, "New Opportunities for Forest Remote Sensing Through Ultra-High-Density Drone Lidar", Surv. Geophys., 40 (4), 959–977, 2019.

[22] M.A. Zulkipli, K.N. Tahar, "Multirotor UAV-Based Photogrammetric Mapping for Road Design", Int. J. Opt., 2018, 1–7, 2018.

[23] A.M. Saad, K.N. Tahar, "Identification of rut and pothole by using multirotor unmanned aerial vehicle (UAV)", Measurement, 137, 647–654, 2019.

[24] S. Jo, B. Lee, J. Oh, J. Song, C. Lee, S. Kim, J. Suk, "Experimental Study of In-Flight Deployment of a Multicopter from a Fixed-Wing UAV", Int. J. Aeronaut. Sp. Sci., 20 (3), 697–709, 2019.

[25] M. Jaud, P. Letortu, C. Théry, P. Grandjean, S. Costa, O. Maquaire, R. Davidson, N. Le Dantec, "UAV survey of a coastal cliff face – Selection of the best imaging angle", Measurement, 139, 10–20, 2019.

[26] B. Kršák, P. Blišťan, A. Pauliková, P. Puškárová, Ľ. Kovanič, J. Palková, V. Zelizňaková, "Use of low-cost UAV photogrammetry to analyze the accuracy of a digital elevation model in a case study", Measurement, 91, 276–287, 2016.

[27] R. Vijayanandh, S. Mano, M. Dinesh, M. Senthil Kumar, G. Raj Kumar, "Design, fabrication and simulation of hexacopter for forest surveillance", ARPN J. Eng. Appl. Sci., 12 (12), 3879–3884, 2017.

[28] H. Zakeri, F.M. Nejad, A. Fahimifar, Rahbin: "A quadcopter unmanned aerial vehicle based on a systematic image processing approach toward an automated asphalt pavement inspection", Autom. Constr., 72 (2), 211–235, 2016.

[29] M. Streßer, R. Carrasco, J. Horstmann, "Video-Based Estimation of Surface Currents Using a Low-Cost Quadcopter", IEEE Geosci. Remote Sens. Lett., 14 (11), 2027–2031, 2017.

[30] J. Liu, J. Lai, P. Lyu, D.D. Lefebvre, B. Jiang, Y. Malang, M. Qu, H.H.T. Liu, Y. Wang, S. Anderson, "Autonomous cyanobacterial harmful algal blooms monitoring using multirotor UAS", Int. J. Remote Sens., 38 (8), 1–26, 2017.

[31] K. Wu, G.A. Rodriguez, M. Zajc, E. Jacquemin, M. Clément, A. De Coster, S. Lambot, "A new drone-borne GPR for soil moisture mapping", Remote Sens. Environ., 235, 111456, 2019.

[32] H. Yao, R. Qin, X. Chen, "Unmanned aerial vehicle for remote sensing applications- A review", Remote Sens., 11 (12), 1443, 2019.

[33] D. Wierzbicki, "Multi-camera imaging system for UAV photogrammetry", Sensors (Switzerland), 18 (8), 2433, 2018.

[34] A. Tripolitsiotis, N. Prokas, S. Kyritsis, A. Dollas, I. Papaefstathiou, P. Partsinevelos, "Dronesourcing: a modular, expandable multi-sensor UAV platform for combined, real-time environmental monitoring", Int. J. Remote Sens., 38 (8), 2757–2770, 2017.

[35] H. Shakhatreh, A.H. Sawalmeh, A. Al-Fuqaha, Z. Dou, E. Almaita, I. Khalil, N.S. Othman, A. Khreishah, M. Guizani, "Unmanned Aerial Vehicles (UAVs): A Survey on Civil Applications and Key Research Challenges", IEEE Access., 7, 48572–48634, 2019.

[36] B. Lillian, Infrared Cameras Inc., "http://www.infraredcamerasinc.com/" (accessed November 24, 2020).

[37] A.M. Pérez Gordillo, J.S.V. Santos, O.D. Lopez Mejia, L.J.S. Collazos, J.A. Escobar, "Numerical and experimental estimation of the efficiency of a quadcopter rotor operating at hover", Energies, 12 (2), 261, 2019.

[38] E. Kuantama, I. Tarca, S. Dzitac, I. Dzitac, R. Tarca, "Flight stability analysis of a symmetrically-structured quadcopter based on thrust data logger information", Symmetry (Basel), 10 (7), 291, 2018.

[39] M.K. Joyo, Y. Raza, S.F. Ahmed, M.M. Billah, K. Kadir, K. Naidu, A. Ali, Z.M. Yusof, "Optimized proportional-integral-derivative controller for upper limb rehabilitation robot", Electron., 8 (8), 826, 2019.

[40] V. Gomez, N. Gomez, J. Rodas, E. Paiva, M. Saad, R. Gregor, "Pareto optimal PID tuning for Px4-based unmanned aerial vehicles by using a multi-objective particle swarm optimization algorithm", Aerospace, 7 (6), 71, 2020.

[41] M.T. Özdemir, D. Öztürk, "Comparative performance analysis of optimal PID parameters tuning based on the optics inspired optimization methods for automatic generation control", Energies, 10 (12), 2134, 2017.

[42] S. Mirjalili, S.M. Mirjalili, A. Lewis, "Grey Wolf Optimizer", Adv. Eng. Softw., 69, 46–61, 2014.

[43] J. Oliveira, P.M. Oliveira, J. Boaventura-Cunha, T. Pinho, "Evaluation of hunting-based optimizers for a quadrotor sliding mode flight controller", Robotics, 9 (2), 1–20, 2020.

[44] Şen MA, Bakırcıoğlu V, Kalyoncu M. "Three Degree of Freedom Leg Design for Quadruped Robots and Fractional Order PID (PiλDμ) Based Control", Konya J Eng Sci, 8(2), 37–47, 2020.

[45] Qu C, Gai W, Zhang J, Zhong M. "A novel hybrid grey wolf optimizer algorithm for unmanned aerial vehicle (UAV) path planning", Knowl. Base Syst., 194 (2), 105530, 2020.